THE USE OF A SECOND-ORDER RECURRENCE RELATION IN THE DIAGNOSIS OF BREAST CANCER

W. T. Hung, A. G. Shannon, and B. S. Thornton
University of Technology, Sydney, NSW 2007, Australia
(Submitted October 1992)

1. INTRODUCTION

The purpose of this paper is to outline an application of number theory in medicine. More specifically, a linear second-order recurrence relation is utilized in a technique for the diagnosis of breast cancer. This continues a tradition in this journal of applications of second-order recurrences. Indeed, the very first issue contained an article by Basin [1] on the Fibonacci sequence in art and nature, and the tradition has been maintained over the years by such authors as Botten [2] who applied the more general sequence of Horadam to a problem in optics. Number theorists, while rightly valuing their work for its beauty and intrinsic worth, are not always aware of the extensive application of the elegant techniques they develop.

In this paper we develop an inhomogeneous linear second-order recurrence relation of the form

$$S_t - B_1 S_{t-1} - B_2 S_{t-2} = B_3 \tag{1.1}$$

for S_t, the relative thermal energy lost by the skin during ultrasonography. (Ultrasonography is a process of visualization of deep structures of the body by recording the echoes of pulses of ultrasonic waves directed into the tissues.) The solutions of (1.1) are then used to distinguish benign and malignant lesions.

The single recurrence relation of the form (1.1) was derived from three interrelated difference equations in a diagnostic model of a breast screening aid (Thornton, Hung, & Hirst [9]). It described the temporal energy changes $S(t)$ $(S_t = S(t)/S(t_0))$ in infrared response of the breast surface when ultrasound is applied to a suspect lesion for an extended time and the results used to evaluate successively the dependent biophysical variables of metabolic energy generated $M(t)$ and the blood perfusion $P(t)$ at each time period. (Perfusion refers to the passage of blood through vessels of a specific organ.) In the present paper an alternative use is made of the three basic difference equations to establish a matrix method which allows S, M, and P to be evaluated at any subsequent time period in one set of matrix operations from the curve fitting to a set of experimental data. This avoids the need for the previous successive dependent calculations at each stage. The biophysical model [9] and clinical background to the project are summarized below in order to appreciate the manner in which the equations arise.

There is a need to minimize biopsies for benign impalpable lesions—those unable to be felt by touch—detected in breast cancer screening programs for healthy women (Hirst & Kearsley [4]). It is the purpose of this project to help reduce unnecessary and potentially harmful interventions into the lives of healthy women yet not miss any malignant cases.

Mammography is currently the only reliable means of detecting breast cancer before a mass can be felt by the act of physical breast examination. More sensitive diagnostic techniques used at early stages of breast cancer, as well as improved management of the disease itself, are now

saving more than half of the women in whom breast cancer is detected at its early stage (Henderson [3]). However, because of the nonspecificity of the mammographic appearance of many malignant lesions, false positives can occur: that is, they are positive on screening but cancer is not subsequently diagnosed. Ultrasonography is used as a complement to mammography because the ultrasound characteristics of malignant lesions are often highlighted in dense parenchyma (the functional elements of an organ) and cystic lesions usually can be differentiated from solid masses.

2. THE BIOPHYSICAL BASIS AND MATHEMATICAL MODEL

Human skin emits infrared radiation, and the total radiated power per unit area, W_T (watts per meter squared per second), is given by

$$W_T = \varepsilon\sigma T^4, \tag{2.1}$$

where ε is the skin's emissivity and T ($^\circ K$) is the temperature of the skin area concerned. (The emissivity is a measure of how well a body can radiate energy; it has a value between 0 and 1.) σ is Stefan's constant, which comes into many biomathematical applications (Reuben & Shannon [8]). The emissivity is approximately unity throughout the spectral region used in infrared thermographic studies. For a local change in skin temperature from $T(t_0)$ at time t_0 to $T(t)$ at time t,

$$W_{T(t)} / W_{T(t_0)} = S(t) / S(t_0) = \left(T(t) / T(t_0)\right)^4. \tag{2.2}$$

Therefore, within a specific spectral range such as the small changes in the breast skin response during sonification of a suspect lesion we can plot the observed values of $T(t) / T(t_0)$ as a convenient basic parameter of thermal energy transfer which permits direct comparisons with S_t calculated from the difference equations of the model described below.

Breast tissue is glandular, fibrous, and fatty, the last of which is the main bulk of the breast. Let U, M, P, and S be, respectively, the ultrasound energy transmitted, the metabolic energy generated, the thermal energy carried away by perfusion and the thermal energy lost by emission from the skin. Figure 1 shows the energy distribution for these variables, which are all functions of time, when diagnostic ultrasound is directed on to the skin in the direction of the suspected lesion.

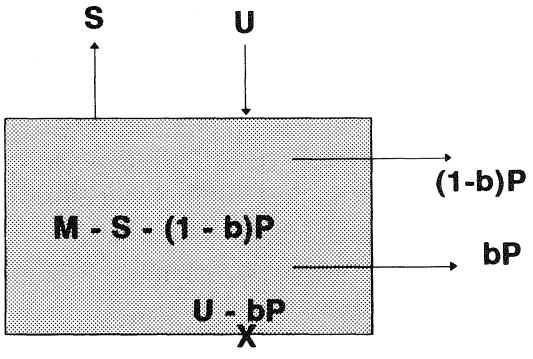

FIGURE 1. The Energy Transfer Diagram

Diagnostic ultrasonography utilizes a frequency range between 1 and 10 million hertz (1×10^6 cycles per second). Such sound waves can only be transmitted in solids and liquids. By way of comparison, a frequency range of 20 to 20,000 cycles per second provides the stimulus for the subjective sensation of hearing [10]. When an ultrasound beam passes through tissue, energy is partly absorbed and converted to heat. This causes a rise in tissue temperature which depends upon several factors such as the heat conduction and transport by blood flow from the exposed tissue into surrounding regions. Figure 2 is a flow diagram to link these energy components.

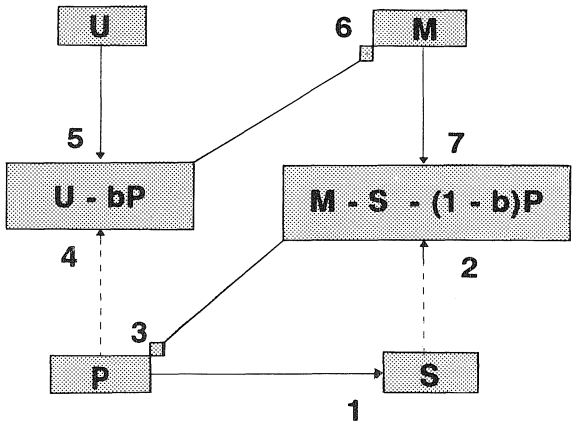

FIGURE 2. The Flow Diagram

If bP represents that part of the ultrasound energy which is absorbed and carried away by perfusion $(0 \le b \le 1)$, then $U - bP$ is the ultrasound energy which reaches the lesion. The perfusion factor b is typically about 0.85 in this sort of work. Since it is generally recognized that there is increased metabolic activity within breast tumors, we can assume that the ultrasound energy received on the lesion will increase the local metabolic activity as formulated in

$$M(t) - M(t-1) = \mu[U(t-1) - bP(t-1)]. \tag{2.3}$$

The metabolic energy that remains after deducting part of it due to the energy lost from the skin and perfusion is $M - S - (1-b)P$. Since increased blood flow is associated with increased metabolic activity (Love, [7]), the increase in perfusion rate is associated with the increase in this remaining metabolic energy as expressed in

$$P(t) - P(t-1) = \lambda[M(t-1) - S(t-1) - (1-b)P(t-1)]. \tag{2.4}$$

Furthermore, skin temperature results primarily from blood perfusion to the tissues and the blood flow in the superficial veins (Love, [7]), as represented by

$$S(t) = aP(t). \tag{2.5}$$

There are two negative feedback loops shown in Figure 2, in which a line with an arrowhead represents a proportional effect and a line with a spearhead represents an integral effect. The proportional effect occurs when a high level of one variable leads to a high level (positive effect indicated by solid line) or low level (negative effect indicated by dotted line) of another variable.

An integral effect is one in which the rate of increase of one variable depends upon the level of another variable. For example, in the loop formed by the lines marked 1, 2, and 3, if P is very high, then S will be very high, but high S will lead to a low value of $M-S-(1-b)P$, which in turn will cause a decrease in P. The second negative feedback loop is formed by lines with heads marked 4, 6, 7, and 3. If P is very high, then $U-bP$ will be low, which will cause a low M and, hence, a low $M-S-(1-b)P$, which in turn will cause a decrease in P.

3. THE DIFFERENCE EQUATION

The three equations (2.3), (2.4), and (2.5) can be combined as follows [9]:

$$\begin{aligned}
a\lambda\mu U(t-2) &= a\lambda M(t-1)-a\lambda M(t-2)+a\lambda\mu bP(t-2) && \text{[from (2.3)]}\\
&= aP(t)-aP(t-1)+a\lambda S(t-1)+a\lambda(1-b)P(t-1)\\
&\quad -aP(t-1)+aP(t-2)-a\lambda S(t-2)-a\lambda(1-b)P(t-2)\\
&\quad +a\lambda\mu bP(t-2) && \text{[from (2.4)]}\\
&= S(t)-S(t-1)+a\lambda S(t-1)+\lambda(1-b)S(t-1)\\
&\quad -S(t-1)+S(t-2)-a\lambda S(t-2)-\lambda(1-b)S(t-2)\\
&\quad +\lambda\mu bS(t-2) && \text{[from (2.5)]}\\
&= S(t)-(2-a\lambda-\lambda(1-b))S(t-1)+(1-a\lambda-\lambda(1-b)+\lambda\mu b)S(t-2).
\end{aligned}$$

Since the ultrasound energy applied at the surface is constant, we set $k=U(t-2)$. For scaling convenience we express $S(t)/S(t_0)$ as S_t, so that we can rewrite the second-order inhomogeneous linear difference equation as

$$S_t-[2-\lambda a-\lambda(1-b)]S_{t-1}-[\lambda a-1+\lambda(1-b)-\lambda\mu b]S_{t-2}=a\lambda\mu k/S(t_0). \tag{3.1}$$

The characteristic equation of this is

$$r^2-[2-\lambda a-\lambda(1-b)]r-[\lambda a-1+\lambda(1-b)-\lambda\mu b]=0, \tag{3.2}$$

from which we get

$$r=\left(2-\lambda a-\lambda(1-b)\pm\sqrt{D}\right)/2, \tag{3.3}$$

where $D=\lambda^2(a-b+1)^2-4\lambda\mu b$. The solutions of the homogeneous part of (3.1) are of the form

$$S_t^{(H)}=\begin{cases} C_1r_1^t+C_2r_2^t & \text{if } D>0,\\ C_1r^t+C_2tr^t & \text{if } D=0,\\ C_1R^t\cos(\theta t)+C_2R^t\sin(\theta t) & \text{if } D<0. \end{cases} \tag{3.4}$$

In the context of the present paper, we note that equations (2.3), (2.4), and (2.5) can also be expressed in matrix form:

$$\begin{bmatrix} 1 & -a & 0\\ 0 & 1 & 0\\ 0 & 0 & 1 \end{bmatrix}\begin{bmatrix} S(t)\\ P(t)\\ M(t) \end{bmatrix}=\begin{bmatrix} 0 & 0 & 0\\ -\lambda & 1-\lambda(1-b) & \lambda\\ 0 & -b\mu & 1 \end{bmatrix}\begin{bmatrix} S(t-1)\\ P(t-1)\\ M(t-1) \end{bmatrix}+\begin{bmatrix} 0\\ 0\\ \mu U(t-1) \end{bmatrix}. \tag{3.5}$$

Now

$$\begin{bmatrix} 1 & -a & 0 \\ 0 & 1 & 0 \\ 0 & 0 & 1 \end{bmatrix}^{-1} = \begin{bmatrix} 1 & a & 0 \\ 0 & 1 & 0 \\ 0 & 0 & 1 \end{bmatrix},$$

so if we let $$V(t) = [S(t),\ \ P(t),\ \ M(t)]^T$$

and $$L = \begin{bmatrix} 1 & a & 0 \\ 0 & 1 & 0 \\ 0 & 0 & 1 \end{bmatrix} \begin{bmatrix} 0 & 0 & 0 \\ -\lambda & 1-\lambda(1-b) & \lambda \\ 0 & -b\mu & 1 \end{bmatrix} = \begin{bmatrix} -\lambda a & a(1-\lambda(1-b)) & a\lambda \\ -\lambda & 1-\lambda(1-b) & \lambda \\ 0 & -b\mu & 1 \end{bmatrix}$$

and $$C = \begin{bmatrix} 1 & a & 0 \\ 0 & 1 & 0 \\ 0 & 0 & 1 \end{bmatrix} \begin{bmatrix} 0 \\ 0 \\ \mu U(t-1) \end{bmatrix} = \begin{bmatrix} 0 \\ 0 \\ \mu U(t-1) \end{bmatrix},$$

then

$$\begin{aligned} V(t) &= LV(t-1) + C \\ &= L^t V(0) + (L^{t-1} + L^{t-2} + \cdots + L + I)C \\ &= L^t V(0) + (L^t - I)(L-I)^{-1} C. \end{aligned}$$

Although this latter expression is algebraically tedious, it can be numerically useful as follows: The first step of fitting S_t to a set of experimental data yields the parameters a, λ and μ (as in the example of Table 1). These parameters can then be used in the above matrix equation to evaluate S, M, and P at any subsequent time period in one set of matrix operations rather than carry out a series of successively interdependent calculations.

4. SOLUTIONS

Horadam and Shannon [5] expound a method for solving equations of the form (3.1). For notational convenience, we let

$$\begin{aligned} B_1 &= 2 - \lambda a - \lambda(1-b), \\ B_2 &= \lambda a - 1 + \lambda(1-b) - \lambda\mu b, \\ B_3 &= a\lambda\mu k / S(t_0), \end{aligned}$$

so that the recurrence relation (3.1) can be rewritten as

$$S_t = \sum_{j=1}^{3} B_j S_{t-j},$$

in which S_{t-3} is treated as though it were unity and $t = 0, 1, \ldots, n$, where $n+1$ is the number of data points. Suppose S_t is the experimental data. The method of least squares is employed to estimate B_j (the estimate of B_j is denoted as $\hat{B}_j$). The sum of squares of errors, SSE, has the form of

$$SSE = \sum_{t=2}^{n} \left(S_t - \sum_{j=1}^{3} B_j S_{t-j} \right)^2. \tag{4.2}$$

By differentiating equation (4.2) with respect to B_i $(i = 1, 2, 3)$ and equating each of them to zero, three normal equations will be obtained, that is,

$$S_{11}\hat{B}_1 + S_{12}\hat{B}_2 + S_{13}\hat{B}_3 = E_1$$
$$S_{21}\hat{B}_1 + S_{22}\hat{B}_2 + S_{23}\hat{B}_3 = E_2$$
$$S_{31}\hat{B}_1 + S_{32}\hat{B}_2 + S_{33}\hat{B}_3 = E_3$$

or

$$S\hat{B} = E, \tag{4.3}$$

where

$$S = \begin{bmatrix} S_{11} & S_{12} & S_{13} \\ S_{21} & S_{22} & S_{23} \\ S_{31} & S_{32} & S_{33} \end{bmatrix}, \quad \hat{B} = \begin{bmatrix} \hat{B}_1 \\ \hat{B}_2 \\ \hat{B}_3 \end{bmatrix}, \text{ and } \quad E = \begin{bmatrix} E_1 \\ E_2 \\ E_3 \end{bmatrix},$$

in which

$$S_{ij} = \sum_{t=2}^{n} S_{t-i}S_{t-j} \quad \text{and} \quad E_i = \sum_{t=2}^{n} S_t S_{t-i} \quad (i, j = 1, 2, 3).$$

Therefore,

$$\hat{B} = S^{-1}E. \tag{4.4}$$

The matrix S is symmetric, so the Choleski-Turing method can find the inverse in an efficient manner (Irving & Mullineux [6]). There are five different situations that can occur depending on the values of D and r in an equation (3.3) and details are given in [9]. As described there, the parameters a, λ, and μ were computed from the equations in Section 4 by fitting the model to the thermal data. The values presented in Table 1 are for several cases for a value of $b = 0.85$ which corresponds to perfusion conditions for a lesion of approximately 5cm below the skin surface.

TABLE 1. Results of Fitting the Model to the Experimental Data Using $b = 0.85$

Patient	Remarks	D	a	λ	μ
A	Benign	1.9828	0.8050	1.6222	0.0757
B	Benign	2.3857	0.8144	2.2098	0.2869
C	Malignant	−1.4888	0.8491	2.7175	0.9589
D	Malignant	−1.2115	0.8409	1.8230	0.7220

5. CONCLUSION

Results from the project suggest that an infrared temporal response measured over an interval of several minutes with simultaneously applied ultrasound stimulation of the suspect region can provide additional information which may help to distinguish between benign and malignant lesions. Where a malignant process is present, a differential cooling pattern occurs in the local skin surface zone prior to recovery to the initial temperature at the skin [9]. Different responses (no recovery) were observed in benign lesions. From the experimental observations so far, it

seems that, if the response curve shows an initial cooling and the fitting of data gives $D < 0$ and $\mu > 0.7$, then it indicates a malignant lesion. The second-order difference equation of the original model [9] reasonably accounts for the thermal changes observed on the skin of the breast, and the matrix method presented here permits improved computational convenience in determining the response, metabolic energy, and perfusion in the successive time periods.

REFERENCES

1. S. L. Basin. "The Fibonacci Sequence as It Appears in Nature." *The Fibonacci Quarterly* **1.1** (1963):53-57.
2. L. C. Botten. "On the Use of Fibonacci Recurrence Relations in the Design of Long Wavelength Filters and Interferometers." *The Fibonacci Quarterly* **20.1** (1982):1-6.
3. J. C. Henderson. "Breast Cancer Therapy—the Price of Success." *The New England Journal of Medicine* **326.26** (1992):1774-75.
4. C. Hirst & J. H. Kearsley. "Breast Cancer Screening: 'One Swallow Doth Not a Summer Make.'" *The Medical Journal of Australia* **154** (1991):76-78.
5. A. F. Horadam & A. G. Shannon. "Asveld's Polynomials $p_j(n)$." In *Applications of Fibonacci Numbers*, Vol. 2, pp. 163-76, ed. A. N. Philippou, A. F. Horadam, & G. E. Bergum. Dordrecht: Kluwer, 1988.
6. J. Irving & N. Mullineux. *Mathematics in Physics and Engineering*, pp. 270-79. New York: Academic Press, 1964.
7. T. J. Love. "Thermography as an Indicator of Blood Perfusion." *Annals of the New York Academy of Sciences* (1980):429-37.
8. A. J. Reuben & A. G. Shannon. "Some Problems in the Mathematical Modelling of Erythrocyte Sedimentation." *IMA Journal of Mathematics Applied in Medicine and Biology* 7 (1990):145-56.
9. B. S. Thornton, W. T. Hung, & C. Hirst. "Diagnostic Model for Local Temporal Thermal Change at the Skin of the Breast during Extended Application of Diagnostic Ultrasound." *IMA Journal of Mathematics Applied in Medicine and Biology* **9** (1992):161-75.
10. G. J. Tortora N. P. Anagnostakos. *Principles of Anatomy and Physiology*, 5th ed., p. 390. New York: Harper & Row, 1987.

AMS Classification Numbers: 11B37, 92C50

❖❖❖